SEMARAK ILMU PUBLISHING

Journal of Advanced Research in Fluid Mechanics and Thermal Sciences

Journal homepage:
https://semarakilmu.com.my/journals/index.php/fluid_mechanics_thermal_sciences/index
ISSN: 2289-7879

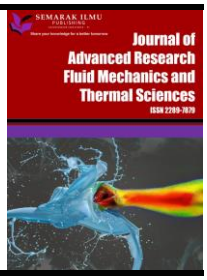

Air Damper Effect on Temperature and Airflow Distribution in Enhancing Thermal Comfort Performance

Nur'Amirah Busu[1], Norasikin Mat Isa[1,*], Azian Hariri[1], Mohamed Hussein[2]

[1] Faculty of Mechanical and Manufacturing Engineering, Universiti Tun Hussein Onn Malaysia, 86400 Parit Raja, Johor, Malaysia
[2] School of Mechanical Engineering, Faculty of Engineering, Universiti Teknologi Malaysia, 81310 Skudai, Johor, Malaysia

ARTICLE INFO

Article history:
Received 12 April 2022
Received in revised form 5 September 2022
Accepted 16 September 2022
Available online 9 October 2022

Keywords:
Airflow distribution; temperature distribution; iris damper; diffuser damper; thermal comfort

ABSTRACT

Heating, ventilating, and air-conditioning (HVAC) technology keeps growing towards providing people with good thermal comfort and indoor air quality. Most buildings use a centralized air-conditioning system in which the air-handling configuration of variable air volume (VAV) system focuses on controlling the zone temperature. But, some of the areas in the zone facing under-actuated and over-actuated airflow lead to the distortion of thermal comfort. Some indoor areas get too cold, and some get too hot due to improper air distribution. The indoor temperature inconsistency will affect the occupants' productivity and work performance. The main focus of this research is to improve the indoor environment's thermal performance by implementing an active air damper as an air controlling device for a centralized air-conditioning system. Indirectly, this will provide the control of temperature for a specific area in the zone with a VAV system. This paper presents the simulation results on the effect of the air damper pattern and its opening parameter against the temperature and airflow distribution in enhancing the thermal comfort performance. The simulation was performed using Ansys FLUENT to analyze three types of air damper patterns: iris, butterfly and radial. The comparison of CFD simulation results shows that the iris damper pattern can provide an acceptable range of temperature of 22 ºC to 24 ºC, which is significant to the desired thermal comfort. The uniform airflow distribution across the indoor area is obtained with no back-flow form in the ducting. Besides, there is a substantial temperature increment when the opening area of inlet airflow is reduced. Therefore, it can be concluded that the iris damper pattern is the best selection for an active air damper since it can provide the best temperature and air flow distribution performance compared to the butterfly and radial air damper.

1. Introduction

The technological development involving heating, ventilation and air-conditioning (HVAC) systems always gains attention for new research and development. A wide range of research fields can be expended in studying the HVAC system, such as the thermal analysis, energy efficiency, control system and the revolution of the HVAC system itself.

* *Corresponding author.*
E-mail address: sikin@uthm.edu.my

https://doi.org/10.37934/arfmts.100.1.152164

A centralized air-conditioning system is one of the commercial HVAC systems widely used in the commercial building. Most buildings implement the variable air volume (VAV) as an air-handling configuration to provide adequate thermal comfort and enhance energy efficiency compared to the constant air volume (CAV) configuration. But still, an under-actuated and over-actuated condition in zones with a VAV system leads to thermal discomfort and energy wastage, thus reducing occupants' productivity and work performance. This problem also had been highlighted by a few authors like Jing *et al.,* [1], Jazizadeh *et al.,* [2] and Zhou *et al.,* [3].

Researchers have proposed various methods to improve a centralized air-conditioning system's indoor thermal performance and energy efficiency. A powerful simulation tool like Ansys FLUENT provides a simple numerical solution for predicting the thermal performance of a building with a reliable result. Buratti *et al.,* [4] performed a CFD simulation to analyze a classroom's indoor condition and thermal comfort. Meanwhile, Popovici *et al.,* [5] successfully simulated the functionality of an HVAC system in an amphitheater during summer and winter. In addition, Mohammed *et al.,* [6] also come out with a suggestion on the optimum thickness of Rockwool insulation in reducing the cooling load and temperature which significantly will reduce the energy consumption.

Not limited to HVAC system analysis, Ansys FLUENT also popular among various field of research. For example, Shandilya *et al.,* [7] used Ansys Fluent to study the air flow and pressure of nozzle. Besides that, Tat *et al.,* [8] managed to determine the correlation impact between the differential pressure to the leakage pipeline and the sound pressure level and turbulence kinetic energy. Meanwhile, Siddharth Jena *et al.,* [9] successfully investigate the effect of environmental wind profile induced due to raised terrains on the pedestrian’s thermal comfort.

Additionally, CFD analysis tools are commonly used in aerospace study. Kai *et al.,* [10] had used 3D CFD simulation to study the power performance of the vertical-axis wind turbine with endplates. Similar with Muhammad Nur Arham Bajuri *et al.,* [11] which study the aerodynamic performance of Savonius Rotor wind turbine based on the blade size and design. Meanwhile, Niknahad *et al.,* [12] had study the comparison of the drag force between circular and triangular vortex generators on the wing of Boeing-737.

Focusing on improving the VAV ventilation system, Millers *et al.,* [13] studied the characteristic of circular air dampers between single blade, iris and conical diaphragm type dampers. He suggested that iris type damper is the most suitable for VAV damper, but more research on precise measurement and control characteristics needs to be done. Meanwhile, Ghofrani et al., [14] also utilized the damper position with minimum airflow and maximum airflow to manipulate the office's indoor temperature. It shows that this method has the potential to improve the energy consumption of HVAC system

Besides that, Jazizadeh *et al.,* [2] proposed an active diffuser in controlling the air supply and direction to maximize thermal comfort and enhance energy efficiency. But the active diffuser will not be effective if the position of occupants keeps changing. Then, Park *et al*., [15] performed a simulation study to analyze the performance of a smart window-integrated (SWV) system in enhancing the indoor air quality and thermal comfort in a single-occupancy office.

Moving towards industrial revolution (IR) 4.0, Table 1 presents the latest technologies and innovations that are currently conducted to improve the thermal performance and enhance the energy efficiency of the HVAC system.

Table 1
The technologies development in HVAC system

Authors	Research Area	Technology Proposed	Findings
Mu *et al.,* [16]	VAV damper	Damper torque airflow sensor	The proposed airflow sensor has a high measurement range ratio of more than 25:1.
Wen *et al.,* [17]	VAV duct	Novel torque damper	It eliminates the coupling effect between local components and achieves accurate air volume monitoring, with an error range of ±5%.
Wang *et al.,* [18]	Multi-zone VAV system	Optimal dynamic duct static pressure (ODSP) method	It provides better energy efficiency with nearly 20% energy saving.
Aftab *et al.,* [19]	Indoor space of a building	Automatic HVAC control with real-time occupancy recognition	An automated HVAC control system achieved over 30% increase in energy saving.
Turner *et al.,* [20]	Residential building	Data-driven automated building HVAC fault detection method	The new fault detection approach has the distinct advantage of being computationally efficient while not requiring a detailed building and HVAC model.
Cetin *et al.,* [21]	Residential and small commercial buildings	On/off controller in EnergyPlus	This method improves around 19% of HVAC energy usage in terms of the Normalized Mean Bias Error (NMBE) at the one-minute level compared to the results without applying the on/off controller.
Dong *et al.,* [22]	Indoor space of a building	Occupancy-based HVAC Control	The occupancy-based HVAC control shows 20% energy saving while still maintaining building comfort requirements.

According to previous research that had been discussed, the diffuser's air damper has not yet been studied. Besides, implementing a control strategy at the diffuser's air damper has not yet been reported and patented. To take this opportunity, the primary objective of this study is to introduce an active diffuser's air damper to enhance thermal comfort while simultaneously improving the energy efficiency of a centralized air-conditioning system with a VAV system.

This paper presents the simulation analysis results on the temperature and airflow distribution performance of a different type of diffuser's air damper patterns in a centralized air-conditioning system. Three types of diffuser air damper are used: iris, butterfly and radial air damper. Selecting the best diffuser's air damper pattern is one of the crucial stages in developing an active air damper.

2. Methodology

2.1 Air Damper Overview

Generally, the diffuser's air damper commonly used in HVAC systems consists of two types which are butterfly and radial damper, as shown in Figure 1(a) and Figure 1(b). Then, the iris damper in Figure 1(c) comes into consideration since the blade pattern provides flexibility in controlling the airflow with uniform distribution. Currently, all these dampers are only available for manual settings. No motorized damper is available for the diffuser's air damper. Since this study is to select the air damper with the best thermal comfort performance, a simulation analysis was conducted to analyze the performance of iris, butterfly and radial damper in terms of temperature distribution and airflow distribution. The numerical simulation was performed using Ansys FLUENT to evaluate the temperature and airflow distribution of each type of air damper pattern.

(a) Butterfly air damper (b) Radial air damper (c) Iris air damper

Fig. 1. Diffuser's air damper patterns

2.2 Simulated Fluid Domain

In the CFD approach, a chamber with a sub-scaled dimension of 1000mm for each width, length and height is selected as the computational fluid domain, as shown in Figure 2. The material assigned for the chamber is Perspex. The chamber was accommodated with a square outlet with 150mm for length, width, and 5mm height, respectively. Meanwhile, a duct and a round diffuser with an inlet diameter of 150mm were placed in the top center of the chamber. The iris, butterfly and radial damper were implemented in the duct with different stages of the opening parameter. Each diffuser's air damper was set to three states of opening parameter, which were maximum, medium and minimum, as shown in Figure 3.

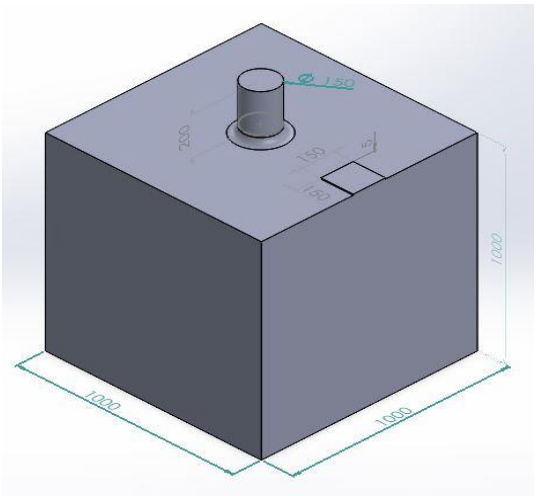

Fig. 2. CFD model domain

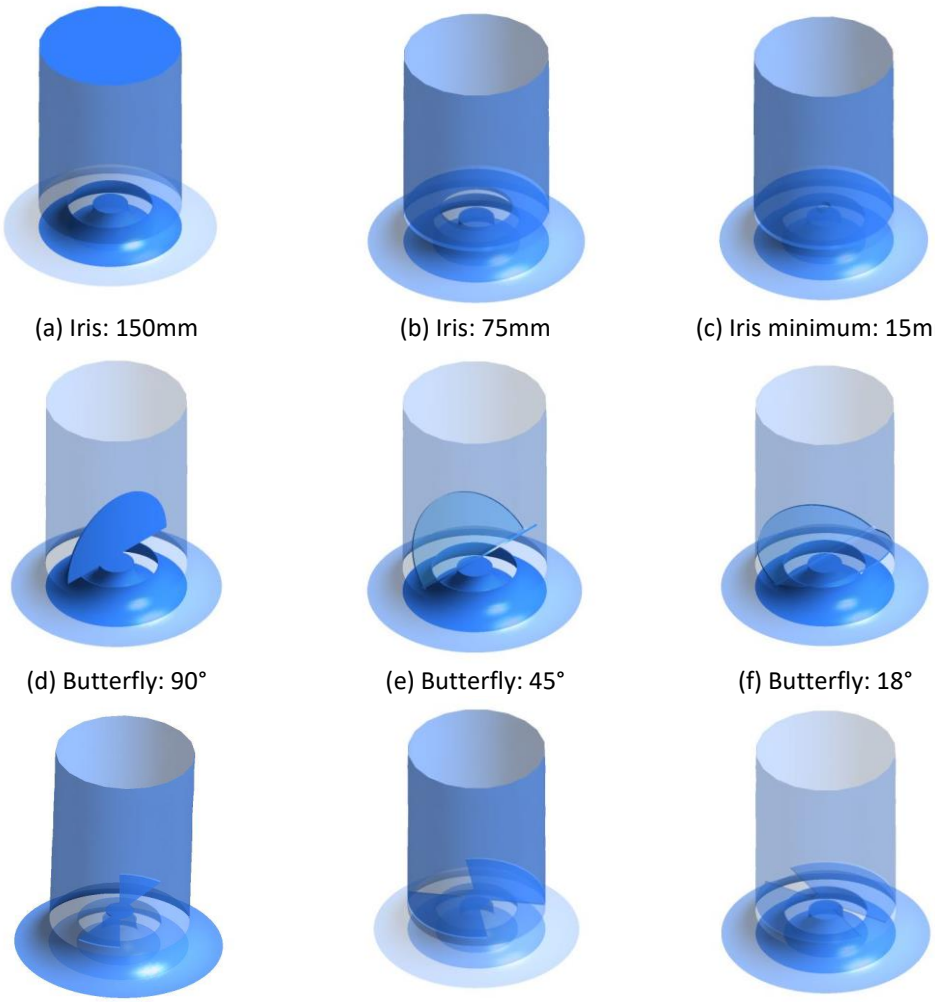

(a) Iris: 150mm (b) Iris: 75mm (c) Iris minimum: 15mm

(d) Butterfly: 90° (e) Butterfly: 45° (f) Butterfly: 18°

(g) Radial:144° (h) Radial: 72° (i) Radial:28.8°

Fig. 3. The illustration with opening parameter for iris, butterfly and radial damper during maximum, medium and minimum opening state

2.3 Grid Independence Test (GIT)

GIT is performed using a parameter set in Ansys FLUENT to obtain a good meshing quality with reliable results. The element size in body sizing was appointed as the input parameter, and the volume-average temperature, skewness and orthogonal mesh quality were set as the output parameter. The element size was adjusted from 50 to 90 with an increment of five to manipulate the number of nodes and ensure the result's independence. Figure 4 shows the GIT result for the iris damper during the minimum opening state. It shows that the body sizing with 65 element size and 118974 nodes can provide a good mesh quality with skewness of 0.8184 and orthogonal quality of 0.1831 compared to other body sizing with an average of 0.84 and 0.15 for the skewness and orthogonal quality, respectively.

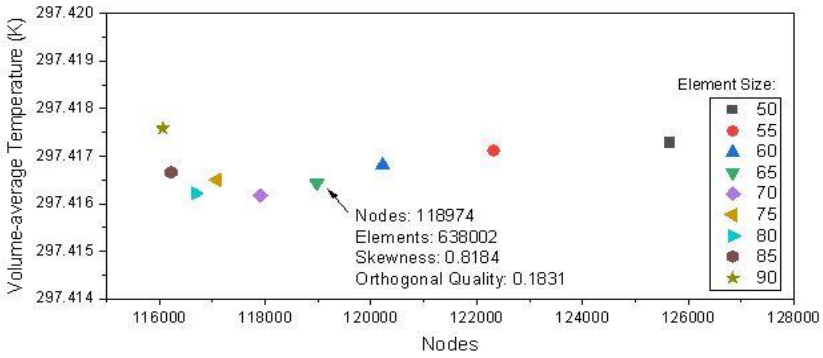

Fig. 4. Grid independency test for iris damper with minimum opening state

The GIT was conducted for each model since the model had a different air damper pattern. The results are selected upon considering the stagnant obtained result along with the meshing quality. A good meshing quality will ensure the convergence of the simulation is obtained. Besides that, the net flux imbalance for the total heat transfer and mass flow rate are -0.0796 w and 2.388e-08 kg/s, less than 1% of the smallest flux through the domain boundary. Thus, it can be confirmed as completely converged.

2.3 Air Flow Model

The Reynold number obtained for the airflow in the ducting was 9548, which is higher than 2300 for internal flow by using Eq. (1),

$$Re = \frac{\rho V d}{\mu} \tag{1}$$

where air density, ρ, air velocity, V, the linear dimension of duct, d, and dynamic viscosity, μ were taken as 1.204 kg/m^3, 1.0 m/s, 0.15 m, and 1.825 ×10^{-5} kg/m.s, respectively. Thus, the airflow in the duct is considered turbulence flow.

In this study, the realizable k–ε turbulence model is selected to simulate the indoor airflow in an insulated chamber with standard wall functions for near-wall treatment. For the indoor environment, the realizable k–ε turbulence model was widely used in the airflow simulation in the HVAC system and provided accurate prediction and reliable results compared to other turbulence models, as discussed by Park *et al.*, [8].

2.5 Numerical Solution

The governing equation of viscous flow, the Navier-Stokes equation for conservation of mass, momentum and energy related to the turbulent reacting flow, was solved using a pressure-based solver with the Coupled algorithm. The general form of the differential equations involved are as follow:

Continuity equation

$$\frac{\partial \rho}{\partial t} + \nabla . (\rho \vec{v}) = S_m \tag{2}$$

Momentum equation

$$\frac{\partial}{\partial t}(\rho\vec{v}) + \nabla.(\rho\vec{v}\vec{v}) = -\nabla\rho + \nabla(\bar{\bar{\tau}}) + \rho\vec{g} + \vec{F} \quad (3)$$

Energy conservation

$$\frac{\partial}{\partial t}(\rho E) + \nabla.\left(\vec{v}(\rho E + \rho)\right) = -\nabla.(\sum_j h_j J_j) + S_h \quad (4)$$

The Least Squares Cell Based approach was used for gradients of solution variables. Meanwhile, second-order upwind was selected for pressure, momentum, turbulent kinetic energy, turbulent dissipation rate and energy in the spatial discretization. The boundary condition implemented in this simulation is shown in Table 2.

Table 2
Boundary conditions.

Boundary	Type	Details
Inlet	Velocity inlet	Velocity: 1m/s Turbulence intensity: 8% Hydraulic diameter: 0.15m Temperature: 18°C
Outlet	Pressure outlet	Default
Duct and Damper	Wall – no slip	Adiabatic condition with zero heat flux
Diffuser	Wall – no slip	Adiabatic condition with zero heat flux
Ceiling	Wall – no slip	Temperature: 27°C
Wall	Wall – no slip	Temperature: 28.5°C
Floor	Wall – no slip	Adiabatic condition with zero heat flux

3. Results

The results are presented comparatively for iris, butterfly and radial damper with the maximum, medium and minimum opening state. Contours of temperature and velocity reveal the qualitative temperature and air flow distribution data. The related temperature and air velocity graphs will be discussed in this section, along with the velocity vector and streamline.

3.1 Temperature Distribution Analysis

The change in temperature distribution due to different types of air damper patterns and opening states is presented in Figure 5. The temperature contours for iris, butterfly and radial air damper were compared at 0.5 m of the x-axis on a 2D plane. The temperature distribution at each air damper's maximum, medium and minimum opening state is observed.

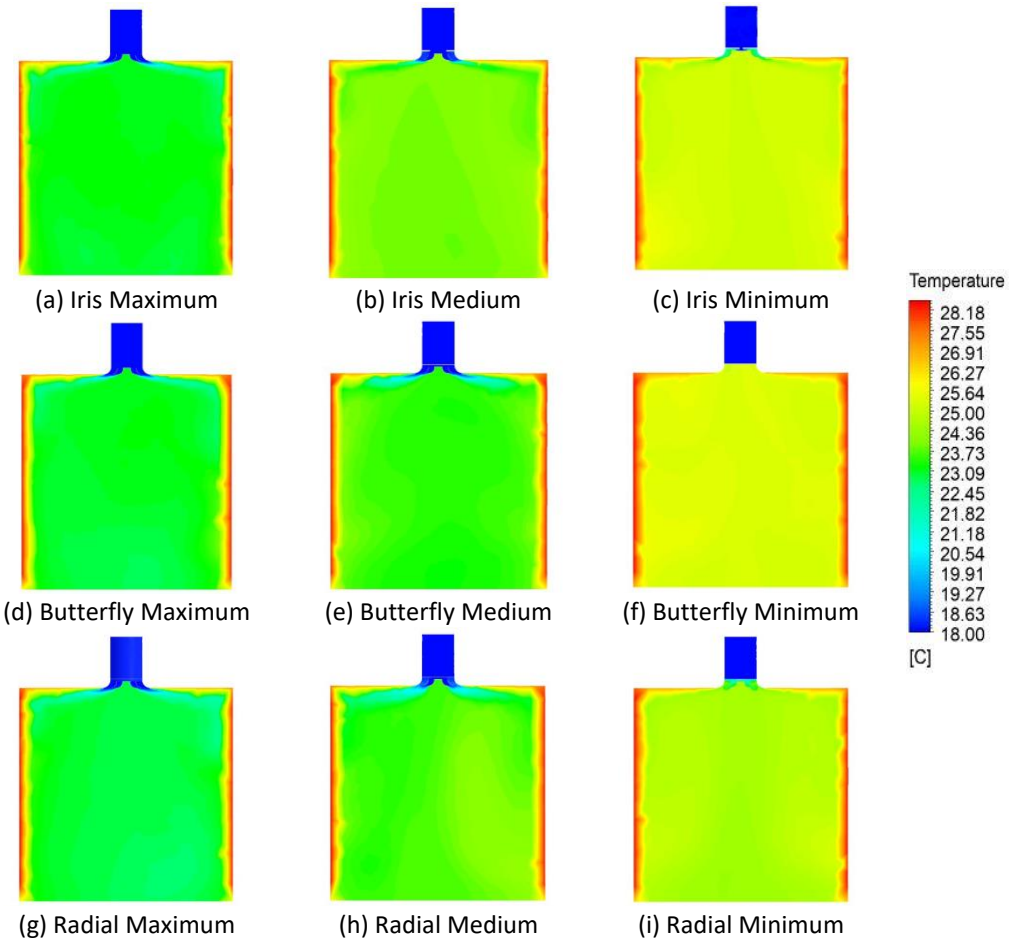

Fig. 5. The comparison of temperature contours for iris, butterfly and radial air damper at maximum, medium and minimum opening state

Generally, the temperature distribution during the maximum opening state of the three air dampers can provide the expected lowest temperature, with the average indoor temperature of 23.15°C. It is aligned with the hypothesis that increasing the inlet airflow's opening area will reduce the indoor temperature. Meanwhile, the indoor temperature is expected to increase when reducing the opening area or airflow inlet.

But, during the medium opening state of the air damper, only the iris damper shows a significant change in indoor temperature with a 0.284% increment in average temperature while maintaining sufficient thermal comfort temperature according to ASHRAE, which is 24°C. Meanwhile, the temperature difference percentage of butterfly and radial air damper is 0.127% and 0.23%, which indicates only slight increments of indoor temperature are achieved even though the opening area of the inlet airflow is reduced to 50%. Besides that, the indoor temperature of both dampers is below the thermal comfort level, as shown in Figure 6.

Figure 7 proved that the iris air damper also achieved a higher temperature during the minimum opening state, which is 26.17°C, compared to butterfly and radial air dampers, which are 25.28°C and 24.6°C, respectively. In fact, changes in the radial air damper's opening conditions cannot significantly change indoor temperature.

Therefore, the iris air damper was successfully proven to manipulate the indoor temperature with changes in the airflow inlet's opening area. Besides that, it can also provide good controllability of the opening diameter of the air damper and good thermal comfort performance of indoor space.

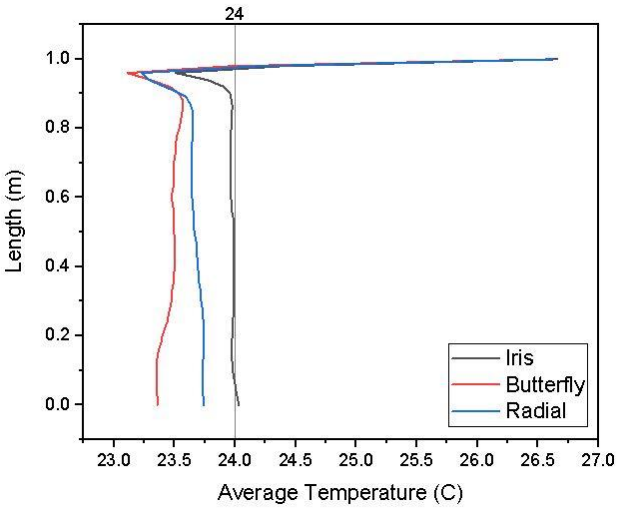

Fig. 6. The comparison of indoor average temperature during a medium opening state of air dampers

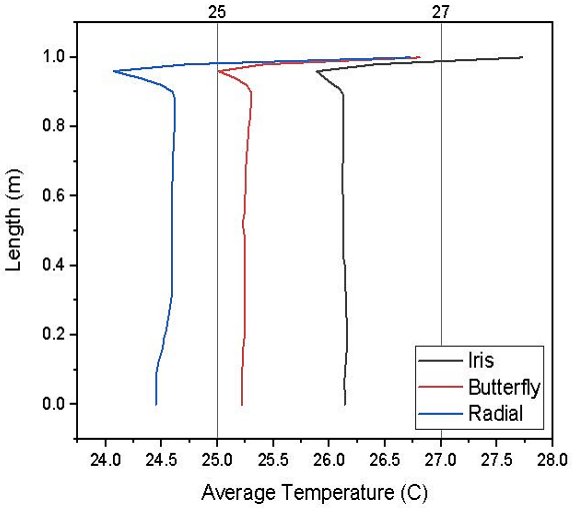

Fig. 7. The comparison of indoor average temperature during a minimum opening state of air dampers

3.2 Airflow Distribution Analysis

Figure 8 visualizes the effect of airflow distribution based on different air damper patterns with various opening states on a 2D plane at 0.5 m of the x-axis. The airflow distribution is revealed with the observation of the velocity contours. The comparison of velocity contours for iris, butterfly and radial air damper shows that the average air velocity in the middle of the room was 0.123 m/s, 0.143 m/s and 0.243 m/s during the maximum, medium and minimum opening state, respectively.

Figure 9 compares the average velocity during the maximum opening state. It shows that the iris and radial air damper show a good agreement in providing better airflow distribution in the indoor space. Meanwhile, the indoor airflow distribution of the butterfly air damper shows a slight distortion.

From Figure 10, it can be seen in the indoor environment of the chamber that the average air velocity is increased when the opening area of the air inlet is reduced. It aligns with the hypothesis that the velocity is higher where the area is smaller. Meanwhile, the average volume air flow rate for iris air damper during the maximum, medium and minimum opening state are 4.68 CFM, 7.16 CFM and 9.52 CFM, respectively.

In addition, airflow distribution is observed with the velocity vector and streamline. During the maximum opening state, all three damper shows a good airflow distribution without any backflow in the duct. Then, during the medium opening state, the iris and radial air damper are able to maintain the thermal and airflow distribution performance. But, backflow of air occurs in the butterfly air damper due to the blade's position, which is 45°, distorting the vertical flow of air, as shown in Figure 11. This same condition was also observed in the minimum opening state.

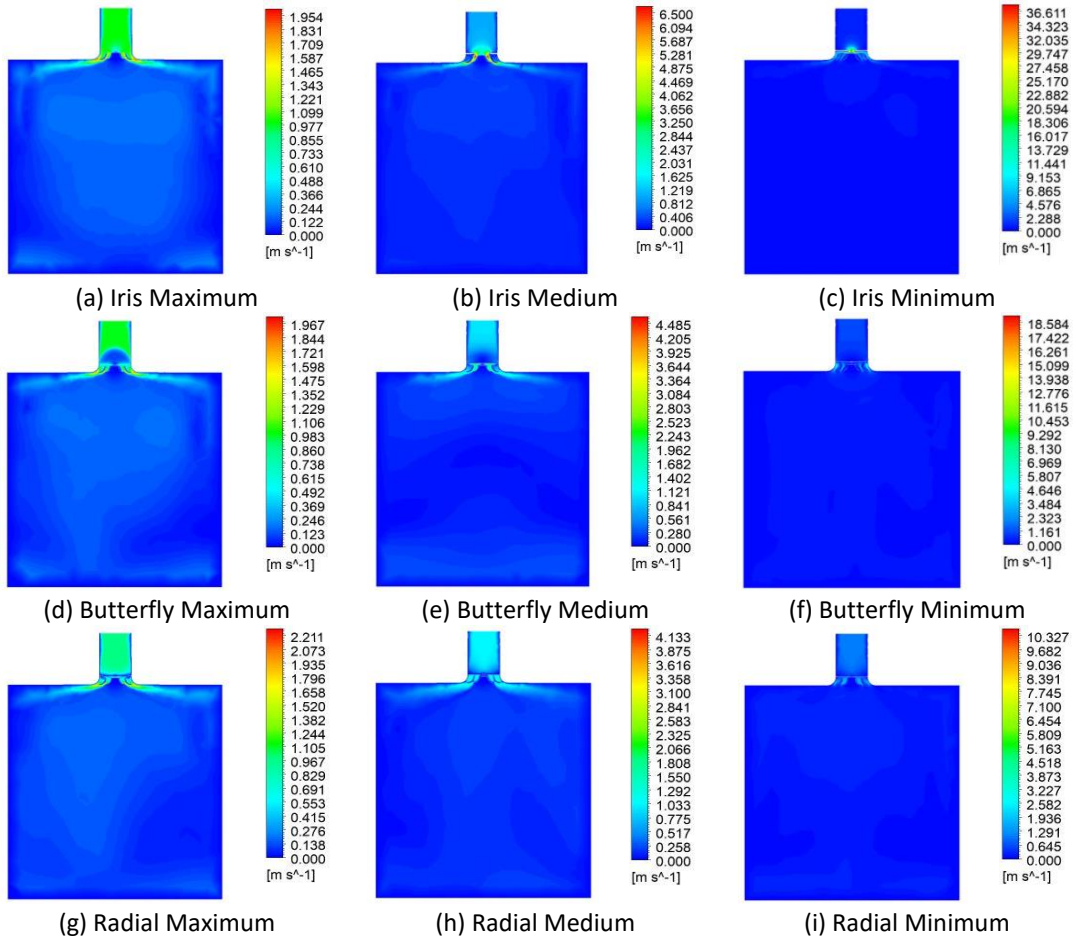

Fig. 8. The comparison of velocity contours for iris, butterfly and radial air damper at maximum, medium and minimum opening state

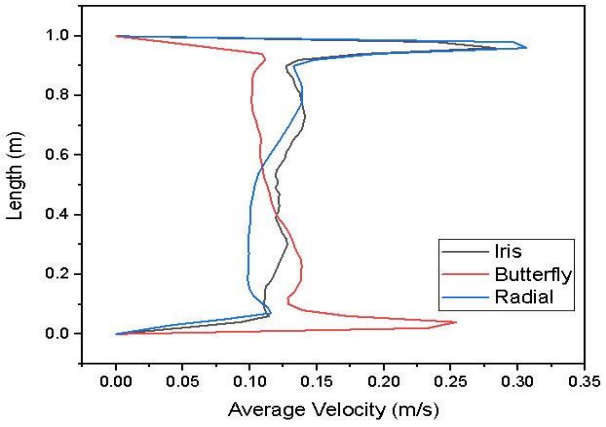

Fig. 9. The comparison of average velocity for iris, butterfly and radial air damper at maximum opening state

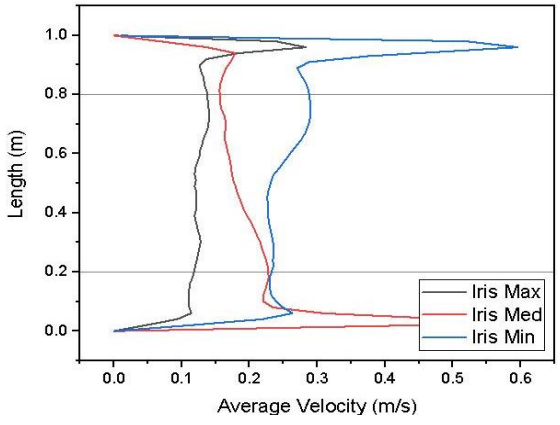

Fig. 10. The comparison of average velocity for iris air damper at maximum, medium and minimum opening state

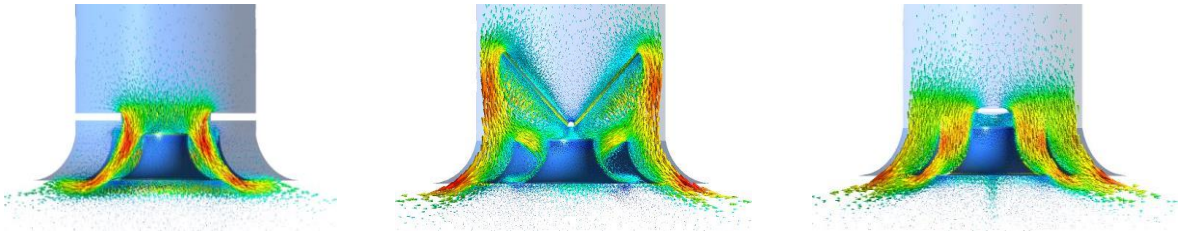

(a) Iris air damper (b) Butterfly air damper (c) Radial air damper

Fig. 11. The comparison of the velocity vector of air damper during a medium opening state

In observing the airflow distribution of the indoor environment, a velocity streamline is used to visualize the uniformity of indoor airflow. The velocity streamlines for each damper pattern were compared. For the minimum opening state of the air damper, the iris damper pattern created more velocity streamline flow in the system. In contrast, the butterfly and radial air damper patterns show the least velocity streamline flow which causes a space uncovered inside the system.

Figure 12 shows the 3D and top view of velocity streamline during the minimum opening state of the iris, butterfly and radial air damper. As expected, the iris air damper can provide a uniform airflow distribution across the indoor space compared to butterfly and radial air dampers. This uniform distribution is significant with the design and opening style of the iris blade.

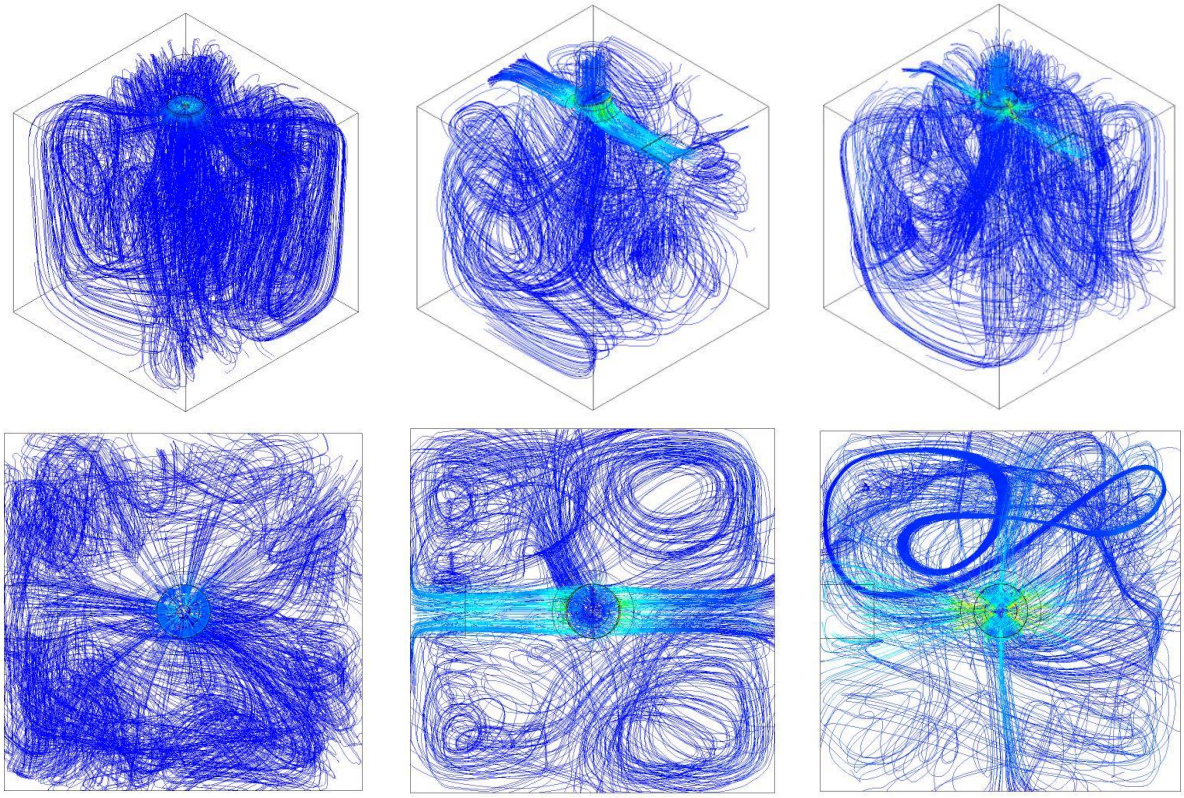

(a) Iris air damper (b) Butterfly air damper (c) Radial air damper

Fig. 12. The comparison of velocity streamlines of air damper during the minimum opening state in three dimension and top view

As we know, the iris air damper manipulates the airflow volume by increasing and reducing the opening diameter of inlet airflow without any obstacle in the middle of the inlet area. Meanwhile, the blade position of the butterfly air damper is in incline condition during opening and closing,

destructing the vertical airflow. The same goes for the radial air damper in which a solid blade is fixed in the middle of inlet airflow.

Therefore, the results obtained in temperature and airflow distribution analysis conducted using Ansys FLUENT proved that an iris air damper could reasonably control temperature and air velocity compared to a butterfly and radial air damper. Besides that, the iris air damper also maintains a good thermal comfort performance of indoor environment and significantly changes air temperature based on the opening state selection.

4. Conclusions

The simulation analysis to study the temperature and airflow distribution of the iris, butterfly and radial air damper pattern was successfully performed using Ansys FLUENT. From the results obtained, it can be concluded that the iris air damper pattern had high potential in maintaining thermal comfort performance with uniform airflow distribution across the indoor space.

Compared to butterfly and radial air damper patterns, the iris air damper pattern met the requirement of an active air damper. Besides providing good performance in temperature and airflow distribution, the iris air damper pattern also shows good agreement in manipulating the indoor temperature by increasing and reducing the inlet airflow diameter. This controllability performance is also crucial in selecting the air damper pattern in developing an active diffuser's air damper.

Therefore, the iris air damper pattern was selected to be implemented in active diffuser's air damper and will be integrated with the thermal control system for further study.

Acknowledgement

The authors would like to thank Universiti Tun Hussein Onn Malaysia (UTHM) and Universiti Teknologi Malaysia (UTM) for their full support of the research work. This work was financially supported by the UTM Research University Grant (RUG) Tier 1 Vot No. 18H28.

References

[1] Jing, Gang, Wenjian Cai, Xin Zhang, Can Cui, Xiaohong Yin, and Huacai Xian. "Modeling, air balancing and optimal pressure set-point selection for the ventilation system with minimized energy consumption." *Applied Energy* 236 (2019): 574-589. https://doi.org/10.1016/j.apenergy.2018.12.026

[2] Jazizadeh, Farrokh, Vedant Joshi, and Francine Battaglia. "Adaptive and distributed operation of HVAC systems: Energy and comfort implications of active diffusers as new adaptation capacities." *Building and Environment* 186 (2020): 107089. https://doi.org/10.1016/j.buildenv.2020.107089

[3] Zhou, Pei, Junqi Wang, and Gongsheng Huang. "A coordinated VAV control with integration of heat transfer coefficients for improving energy efficiency and thermal comfort." *Energy Procedia* 143 (2017): 271-276. https://doi.org/10.1016/j.egypro.2017.12.683

[4] Buratti, Cinzia, Domenico Palladino, and Elisa Moretti. "Prediction of indoor conditions and thermal comfort using CFD simulations: A case study based on experimental data." *Energy Procedia* 126 (2017): 115-122. https://doi.org/10.1016/j.egypro.2017.08.130

[5] Popovici, Cătălin George. "HVAC system functionality simulation using ANSYS-Fluent." *Energy Procedia* 112 (2017): 360-365. https://doi.org/10.1016/j.egypro.2017.03.1067

[6] Muhieldeen, Mohammed W., Lim Chong Lye, M. S. S. Kassim, Tey Wah Yen, and K. H. Teng. "Effect of Rockwool Insulation on Room Temperature Distribution." *Journal of Advanced Research in Experimental Fluid Mechanics and Heat Transfer* 3, no. 1 (2021): 9-15.

[7] Shandilya, Anuj, and Suranjana Gangopadhyay. "New Designed Main Nozzle of Air-Jet Weaving Machine for Optimizing Air Consumption using CFD Simulation." *CFD Letters* 14, no. 9 (2022): 108-117. https://doi.org/10.37934/cfdl.14.9.108117

[8] Tat, Toh Wei, Norzelawati Asmuin, Ishrizat Taib, and Riyadhthusollehan Khairulfuaad. "Acoustic Pressure Simulation for Fluid Piping Leakages." *CFD Letters* 14, no. 7 (2022): 77-86. https://doi.org/10.37934/cfdl.14.7.7786

[9] Jena, Siddharth, and Ajay Gairola. "Novel Boundary Conditions for Investigation of Environmental Wind Profile Induced due to Raised Terrains and Their Influence on Pedestrian Winds." *Journal of Advanced Research in Applied Sciences and Engineering Technology* 27, no. 1 (2022): 77-85. https://doi.org/10.37934/araset.27.1.7785
[10] Khai, Tan Chun, Ahmad Faiz Mohammad, Ahmad Fazlizan, Sheikh Ahmad Zaki, and Farah Liana Mohd Redzuan. "Numerical Investigation of the Power Performance of the Vertical-Axis Wind Turbine with Endplates." *CFD Letters* 14, no. 6 (2022): 90-101. https://doi.org/10.37934/cfdl.14.6.90101
[11] Bajuri, Muhammad Nur Arham, Djamal Hissein Didane, Mahamat Issa Boukhari, and Bukhari Manshoor. "Computational Fluid Dynamics (CFD) Analysis of Different Sizes of Savonius Rotor Wind Turbine." *Journal of Advanced Research in Applied Mechanics* 94, no. 1 (2022): 7-12.
[12] Niknahad, Ali. "Numerical study and comparison of turbulent parameters of simple, triangular, and circular vortex generators equipped airfoil model." *Journal of Advanced Research in Numerical Heat Transfer* 8, no. 1 (2022): 1-18.
[13] Millers, Renars, and Uldis Pelite. "Survey of control characteristics of circular air dampers in variable air volume ventilation systems." *Energy Procedia* 96 (2016): 294-300. https://doi.org/10.1016/j.egypro.2016.09.152
[14] Ghofrani, Ali, Seyyed Danial Nazemi, and Mohsen A. Jafari. "Prediction of building indoor temperature response in variable air volume systems." *Journal of Building Performance Simulation* 13, no. 1 (2020): 34-47. https://doi.org/10.1080/19401493.2019.1688393
[15] Park, Dong Yoon, and Seongju Chang. "Effects of combined central air conditioning diffusers and window-integrated ventilation system on indoor air quality and thermal comfort in an office." *Sustainable Cities and Society* 61 (2020): 102292. https://doi.org/10.1016/j.scs.2020.102292
[16] Mu, Yuanpeng, Mingsheng Liu, Zhixian Ma, and Jili Zhang. "Resistance characteristic analysis based study on a novel damper torque airflow sensor for VAV terminals." *Building and Environment* 175 (2020): 106813. https://doi.org/10.1016/j.buildenv.2020.106813
[17] Wen, Shihao, Junjie Liu, Fan Zhang, and Jing Xu. "Numerical and experimental study towards a novel torque damper with minimized air flow instability." *Building and Environment* 217 (2022): 109114. https://doi.org/10.1016/j.buildenv.2022.109114
[18] Wang, Xuetao, Qianchuan Zhao, Yifan Wang, and Tian Xing. "Optimal Dynamic Duct Static Pressure Method in a Multi-Zone Variable Air Volume System." *IEEE Robotics and Automation Letters* 6, no. 3 (2021): 5969-5975. https://doi.org/10.1109/LRA.2021.3089135
[19] Aftab, Muhammad, Chien Chen, Chi-Kin Chau, and Talal Rahwan. "Automatic HVAC control with real-time occupancy recognition and simulation-guided model predictive control in low-cost embedded system." *Energy and Buildings* 154 (2017): 141-156. https://doi.org/10.1016/j.enbuild.2017.07.077
[20] Turner, W. J. N., A. Staino, and B. Basu. "Residential HVAC fault detection using a system identification approach." *Energy and Buildings* 151 (2017): 1-17. https://doi.org/10.1016/j.enbuild.2017.06.008
[21] Cetin, Kristen S., Mohammad Hassan Fathollahzadeh, Niraj Kunwar, Huyen Do, and Paulo Cesar Tabares-Velasco. "Development and validation of an HVAC on/off controller in EnergyPlus for energy simulation of residential and small commercial buildings." *Energy and Buildings* 183 (2019): 467-483. https://doi.org/10.1016/j.enbuild.2018.11.005
[22] Dong, Jin, Christopher Winstead, James Nutaro, and Teja Kuruganti. "Occupancy-based HVAC control with short-term occupancy prediction algorithms for energy-efficient buildings." *Energies* 11, no. 9 (2018): 2427. https://doi.org/10.3390/en11092427